CHARACTERIZATION OF ZrB_2-SiC COMPOSITES WITH AN ANALYTICAL STUDY ON MATERIAL REMOVAL RATE AND TOOL WEAR RATE DURING ELECTRICAL DISCHARGE MACHINING

S. Sivasankar[1] and R. Jeyapaul[2]
[1]*Department of Mechanical Engineering, Government College of Engineering, Thanjavur, Tamilnadu, India*
[2]*Department of Production Engineering, National Institute of Technology, Tiruchirappalli, Tamilnadu, India*
E-mail: shivasankar09@gmail.com, jeyapaul@nitt.edu

Received August 2015, Accepted February 2016
No. 15-CSME-90, E.I.C. Accession 3855

ABSTRACT
This research work concentrates on Electrical Discharge Machining (EDM) performance evaluation of ZrB_2-SiC ceramic matrix composites with different tool materials at various machining parameters. Monolithic ZrB_2 possesses lower relative density (98.72%) than composites. ZrB_2 with 20 Vol.% of SiC possesses 99.74% of the relative density with improved hardness values. Bend strength and Young's modulus increase with SiC addition until it reaches 20 Vol% and then decreasing. EDM performance on tool materials of tungsten, niobium, tantalum, graphite and titanium at various levels of pulse on time and pulse off time are analyzed. Graphite produces the best Material removal rate (MRR) for all the workpieces. Tool wear rate decreases with melting point and thermal conductivity of the tool material.

Keywords: ceramic machining; CMC; composite machining; ZrB_2; SiC; EDM.

DESCRIPTION DES COMPOSITES ZrB_2-SiC ET ÉTUDE ANALYTIQUE DU TAUX D'ENLÈVEMENT DE LA MATIÈRE ET LE TAUX D'USURE DES OUTLS PENDANT L'USINAGE PAR ÉLECTRO-ÉROSION

RÉSUMÉ
Le présent travail de recherche se concentre sur l'évaluation de la performance d'usinage par électro érosion (EDM) d'un matériau composite à matrice céramique ZrB_2-SiC avec différents matériaux d'outils et paramètres d'usinage variés. Les matériaux monolithiques ZrB_2 ont une densité relative plus basse (98.72%) que les composites. Les matériaux ZrB_2 comportant 20% de masse volumique de carbure de silicium (SiC) ont 99.74% de relative densité et des valeurs améliorées de dureté. La force de flexion et le module de Young augmentent avec l'addition de SiC jusqu'à ce qu'il atteigne 20% de masse volumique pour aller en décroissant. Nous analysons la performance de l'usinage par électro-érosion (EDM) sur les matériaux d'outils en tungstène, niobium, tantale, graphite, et titane à différents niveaux de temps d'enclenchement d'impulsion et de déclenchement. Le graphite possède le meilleur taux d'enlèvement de matière pour toutes les pièces. L'usure des outils diminue avec le point de fusion et la conductivité thermique du matériel de l'outil.

Mots-clés : usinage de la céramique; CMC; usinage des composites; ZrB_2; SiC; EDM.

1. INTRODUCTION

Most of the studies on pure ZrB_2 or ZrB_2-SiC have concentrated on investigating resistance to oxidation and properties. Very little attention has been paid to the machining of these materials in spite of the importance of that aspect to ensure the use of these materials on high temperature nozzle applications. Thus, there is a lack of systematic machinability studies as a function of the volume proportions of constituent. In recent times, this is being considered for use as potential candidates for a variety of high-temperature structural applications, including furnace elements, plasma-arc electrodes, or rocket engines and thermal protection structures for leading-edge parts on hypersonic re-entry space vehicles at over 1800°C [1]. Though it has the potential use in high temperature regions, the end product cannot always be produced directly through powder metallurgy route; it needs some additional processing like machining. So, machining is an inevitable requirement to produce complex and precision components of structural ceramics so that the area of its application can be widened. Due to high hardness and strength of Ultra High Temperature Ceramics (UHTC) machining cost of this component accounts for an important percentage of the final cost.

The use of diamond tools and some special processing technologies such as laser machining and ultrasonic machining are often inefficient and costly, though those processes make some hard ceramic materials machinable [2]. Since there is no direct contact between the tool and the workpiece, no mechanical stress has been developed either in the workpiece or in the tool. Workpieces can be machined under EDM as long as they are electrically conductive. As a result, EDM is often used to machine high strength or hard materials [3]. Dry EDM has characteristics of high material removal rate and low tool wear ratio. Hence, dry EDM is suitable for three-dimensional milling of difficult-to-cut materials, such as cemented carbide [4].

In general materials employed at very high temperatures are expected to be not only light but also be physically stable and chemically non reactive over 1600°C. Ceramic materials are able to fulfill these requirements in cyclic and prolonged conditions. For these reasons there is an unprecedented demand for UHTCs. Zhu et al. [5] shows that Hf and Ta alloys were discarded in spite of having an acceptable resistance to oxidation because of the limitations imposed by their low melting point of only 2000°C. Zhang et al. [6] and Wang et al. [7] stated that components of the Ir-C system are insufficiently refractory due to the existence of a eutectic point at 2296°C. Lawn [8] and Suryanarayana [9] show that the materials of C-C, C-SiC and SiC-SiC systems have very good mechanical properties at high temperatures, but very least resistance to oxidation. While all these options have been analyzed, research made in the last few years has allowed the recognition of the diboride of metals of the IVb group (i.e., Zr, Hf) as the most hopeful UHTCs. Ceramic materials are extensively used in the industrial fields that produce cutting tools, self-lubricating bearings, nozzles, turbine blades, internal combustion engines, and heat exchangers [10]. ZrB_2 and hafnium diboride (HfB_2) are considered to be the most representatives of the ultra-high temperature ceramics, due to their excellent combination of high melting point, hardness, wear resistance and good chemical inertness [11]. Fahrenholtz et al. [12] stated that these superb features make them attractive candidates for high temperature applications where thermal, erosion, chemical and wear resistance are required, such as refractory materials in foundries, electrical devices and metallurgy. Chamberlain [13] reported the flexural strength increases from 550 MPa for pure ZrB_2 to 1100 MPa for ZrB_2-30 Vol.% SiCp. Likewise, fracture toughness ranged from 3.5 to 5.3 MPa $m^{1/2}$ over the same composition range. Tripp et al. [14] addressed the effect of a SiC addition on the oxidation of ZrB_2. The oxidation resistance of ZrB_2 can be accomplished with the addition of 10–30 Vol.% SiC particulates as a second phase. Tripp proved that the densification properties started getting improved severely from 15% onwards [14]. The benefits of adding SiC to ZrB_2 is discussed by Hwang (2007) who stated that there are three benefits of adding SiC to ZrB_2. SiC acts as a sintering aid, facilitating densification at lower temperatures. SiC provides ZrB_2 with greater oxidation and ablation resistance, and SiC improves the thermo-mechanical properties relevant for the aerospace applications proposed for ZrB_2 [15].

The high strength, combined with high room temperature thermal conductivity (60 W/mK^2), indicates the potential for good thermal shock resistance. The high electrical conductivity of ZrB_2 (108 S/m) is sufficient for EDM allowing for relatively low cost machining of complex components [16]. Monteverde [17] made a comparative study on EDM of ZrB_2 + 15 SiC and ZrB_2 + SiC + 10 HfB_2 and stated that R_a is 0.6 μm for ZrB_2 + 15 SiC and 1 μm for ZrB_2 + SiC + 10HfB_2, R_z is 4.9 μm, and 7.5 μm for these two materials respectively.

Influences of pulsed power condition on the machining properties in micro EDM was studied by Seong Min Son et al. [18] and then proposed that voltage, current, and pulse on/off time of the EDM power are the main parameters to make a decision of the material removal rate. Voltage and current are proportional to the material removal rate. The gap between a tool and a machined surface is increased with an increase of voltage and current. Pulse on time and off time are the most significant factors in EDM machining; so these two factors are considered for analysis [19]. Tool material plays a major role in Material removal rate so that it is categorized as the important non-electric parameters in EDM [20].

In this study, the performance of the tool materials at various levels of pulse on time and pulse off time are analyzed while machining of ZrB_2-SiC composites based on material removal rate. Positive polarity is selected by keeping constant peak current and voltage with different levels of pulse on time and pulse off time. No rotational speed is given to the tool. During machining, a constant feed in the vertically downward direction along the Z axis has been given.

The workpiece material of ZrB_2-SiC composite (15, 20, 25 & 30 Vol.% of SiC with ZrB_2) are manufactured in the shape of discs by means of a hot pressing technique and this disc is machined using diamond load grinding to make them parallel surfaces. The characterization analysis is conducted to study the density, bend strength, fracture toughness, SEM analysis, and powder morphology behavior.

Holes with a diameter of 2 mm are machined on the disc using EDM spark erosion machine with different tool materials. Machinability studies on ZrB_2-SiC composites through EDM using the electrode materials of tungsten, niobium, tantalum, graphite and titanium has been carried out.

2. WORKPIECE PREPARATION

The workpiece for this study is manufactured through powder metallurgy route. This process conserves energy and raw materials, minimizes pollution and machining in comparison to other manufacturing technologies ensuing in reduced costs. Another attraction of the process is the ability to fabricate high quality complex parts to close tolerances from high performance and specialty materials in an economical manner. The powder for this workpiece preparation is procured from different manufacturers, and the powder specifications are shown in Table 1.

Table 1. Size, grade and manufacturer of starting powders.

Starting Powder	Particle Size (μm) – D_{50}	Grade/Manufacturer	Purity(from manufacture assay)
ZrB_2	1.5–3.0 μm	Grade B, HC Stark ABCR GmbH & Co., Germany	B – min 18.5% C – max 0.2%, O – max 1.5% N – max 0.25%, Fe – max 0.1% Hf – min 0.2%
B_4C	7–8 μm	Electro Abrasives Corporation, USA	N – 0.44%, O – 1.34%, Fe – 0.03%, Si – 0.05%, Al – 0.01%
SiC	2.5 μm	Electro Abrasives Corporation, USA	SiC – 99.5%, SiO_2 – 0.2%, Si – 0.03%, Fe – 0.04%, C – 0.1%

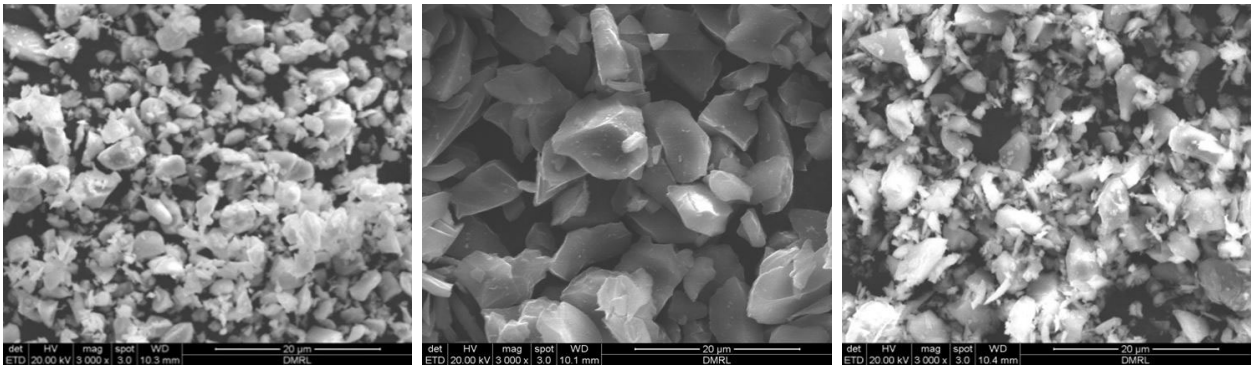

Fig. 1. (a) SEM picture of ZrB_2 powder; (b) SEM picture of B_4C powder; (c) SEM picture of SiC powder.

2.1. Powder Characterization

The powders namely ZrB_2, B_4C and SiC were examined by Scanning Electron Microscope (SEM) and the micrograph pictures were shown in Figs. 1a, b and c respectively. Further, the particle sizes of the powders are analyzed using Microtrac Blue wave Particle Size Analyzer with Tri-laser Technology. Zirconium Diboride possesses hexagonal crystal phase with high melting point (3040°C), high hardness, high thermal conductivity, good electrical conductivity, stable in a wide temperature range, good oxidation resistance in air, and good anti-corrosion ability. Figure 1a shows the SEM micrograph of ZrB_2. The micrograph portrays the relatively fine particle structure of ZrB_2 compared to B_4C and SiC. The presence of thin flakes further justifies the fineness of the powder. The average particle size of the ZrB_2 powder is 2.69 ± 1.26 μm.

Boron Carbide is one of the hardest materials known, ranking third behind diamond and cubic boron nitride. Boron carbide has a complex crystal structure typical of icosahedrons-based borides. It possesses high melting point (2445°C), extreme hardness, low density, good chemical resistance and nuclear properties. The SEM micrograph shows particles with large surface area. The average particle size of B_4C powder is 6.05 ± 2.73 μm which is relatively larger than the other two powders.

Silicon carbide is composed of tetrahedral of carbon and silicon atoms with strong bonds in the crystal lattice. SiC possesses high melting point (2730°C), Low density, high strength, high hardness and excellent thermal shock resistance. The SEM micrograph depicts the presence of powder and flakes with some amount of whiskers. The average particle size of SiC powder is found to be 3.15 ± 1.18 μm.

2.2. Powder Synthesis

Initially the powder of measured quantity is ball milled for 2 to 3 hrs. The alumina balls are used as a milling media. For initial study on monolithic, 0.4 weight % of B_4C was added as a densification agent. This powder mixture with equal weight of alumina balls of 5 mm diameter was filled in polythene bottles with ethanol as a mixing agent. Each bottle was closed with an air tight cork. Then all the bottles were placed inside a cylindrical china clay pot. The gaps between the bottles were closely packed with charcoal so that an individual bottle will not rotate on its own. The pot was placed over the parallel shafts of unidirectional rotation. The axis of the pot and the rotors shaft were parallel to each other. Due to the gravitational force, the pot did not require additional clamping. The rotational speed of the pot was maintained at 200 rpm. This milling was carried out for 24 hrs. Similarly ZrB_2-SiC composites with four different volume proportions like 70% ZrB_2-30% SiC, 75% ZrB_2-25% SiC, 80% ZrB_2-20% SiC, 85% ZrB_2-15% SiC were ball milled. The milled powder mixture was dried in air. Finally it was hot pressed.

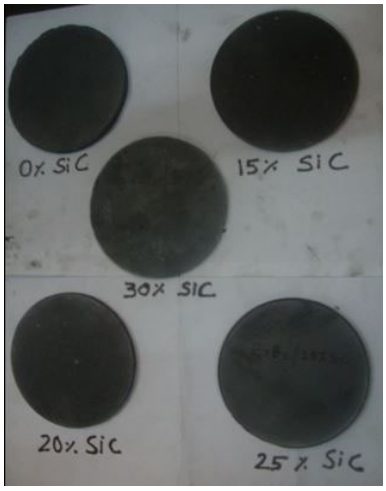

Fig. 2. Photographic image of the workpieces.

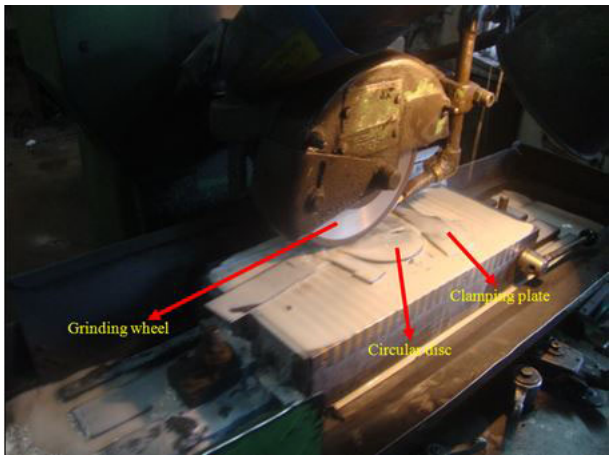

Fig. 3. Grinding of the workpiece.

2.3. Hot pressing Process

Monolithic ZrB_2 and ZrB_2-SiC composites were hot pressed in an organ atmosphere to a disc of 100 mm diameter and 5 mm thickness. The temperature during pressing was maintained at 2000°C with a pressure of 30 MPa. The compaction was done for a period of 60 min [2]. The photographic images of the hot pressed discs are shown in Fig. 2.

2.4. Sand Blasting and Grinding

The hot pressed disc surfaces do not have uniform surfaces and may contain graphite particles. In order to rectify this problem, these discs were subjected to sand blasting process. After this, the disc was subjected to diamond load grinding (Grinding wheel dia. 175 mm, grit size 126, rotates at, 3600 rpm) until it reaches the coplanar surfaces. This is shown in Fig. 3. Finally the disc reaches a thickness of 4.2 mm. A square block of size 65 mm is engraved from the disc using WEDM process to facilitate clamping positional accuracy of the hole. Figure 4 shows the square shaped workpiece.

Fig. 4. Workpiece after grinding and square cut.

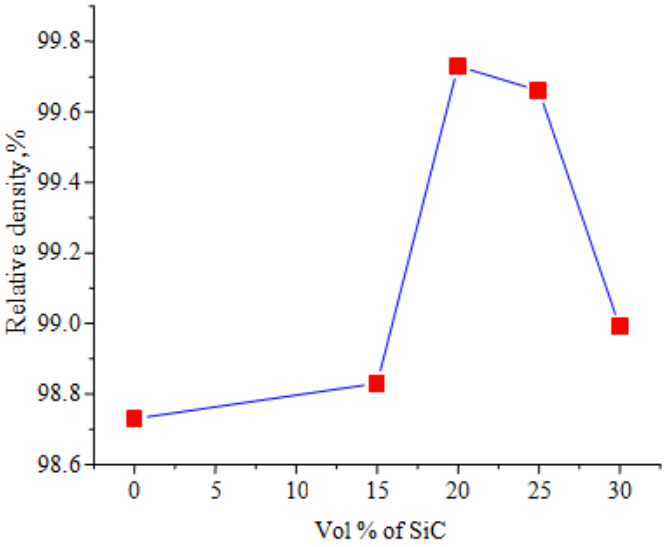

Fig. 5. Relative density of composite with different Vol.% of SiC.

3. WORKPIECE CHARACTERIZATIONS

3.1. Densification Behaviour

In this work, the density of the hot pressed component is calculated through Archimedes' principle, which reads as when an object is immersed in a fluid, the fluid exerts on the object a force whose magnitude is equal to the weight of the displaced fluid and whose direction is opposite to the force of gravity. Figure 5 shows the density variation of the monolithic ZrB_2 and ZrB_2-SiC composites. In general, the entire specimen shows good density behaviour and, in particular, composites possess better density behaviour than monolithic due to the hindering nature of SiC. Monolithic ZrB_2 possesses lower density than composites do. Improvement of densification, due to addition of SiC, is documented in the literature. The addition of SiC produces an intergranular liquid phase that favours the process of grain rearrangement as well as improves the packing. It is confirmed that the addition of SiC remarkably inhibited grain growth of the ZrB_2 matrix. The grain size of the ZrB_2 matrix decrease with increasing SiC content. The least grain size is attained for ZrB_2 with

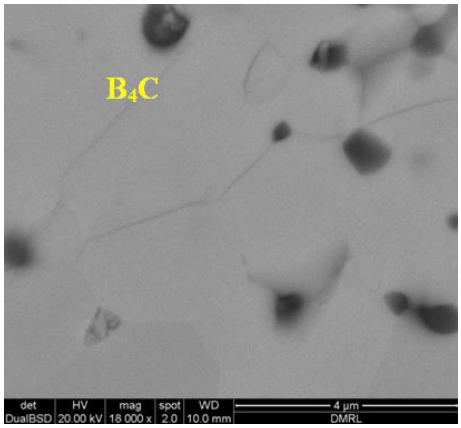

Fig. 6. SEM picture of monolithic ZrB_2.

20 Vol.% SiC composite. When the SiC content increases up to 20 Vol.%, the number of intragranular SiC particles will increase markedly which causes an increase in density. Beyond an SiC content of 20 Vol.% (up to 30 Vol.%), because of the disappearance of the intragranular microstructure which results from the unusual growth of SiC, this leads to a decrease in the density [21].

3.2. Microstructures Study

Figure 6 shows the SEM image of monolithic ZrB_2 and it reveals that B_4C (0.5 weight%) is uniformly distributed on ZrB_2 phase. Micro cracks are also observed. Figures 7a–d give the SEM details of 85% ZrB_2-15% SiC, 80% ZrB_2-20% SiC, 75% ZrB_2-25% SiC, 70% ZrB_2-30% SiC respectively. These images assure the uniform distribution SiC (reinforcing phase) over ZrB_2 (matrix) phase.

3.3. Hardness Behaviour

The micro hardness test was conducted with a load of 0.25 kgf. Vickers diamond pyramid is used as the indenter. The procedure for testing is very similar to that of the standard Vickers hardness test, except that it is done on a microscopic scale with higher precision instruments. Precision microscopes are used to measure the indentations; these microscopes usually have a magnification of around X500 and measure to an accuracy of +0.5 micrometers. Also, with the same observer differences of +0.2 micrometers can usually be resolved. Vickers harness of the specimens is shown in Fig. 8. Since the hardness of SiC is greater than that of ZrB_2, the increment in hardness while increase in contribution of SiC is not anonymous. The hardness linearly varies with the volume % of SiC with almost constant slope. But the value of this slope is lower for monolithic ZrB_2.

3.4. Bend Strength and Elastic Modulus

To study the flexural strength of these composites, a three point bend test was performed on different composite samples at room temperature using Instron 5500 R universal testing machine. The testing conditions are as follows:

Length of span: 40 mm

Maximum load: 10 KN

Crosshead Speed: 0.5 mm/min.

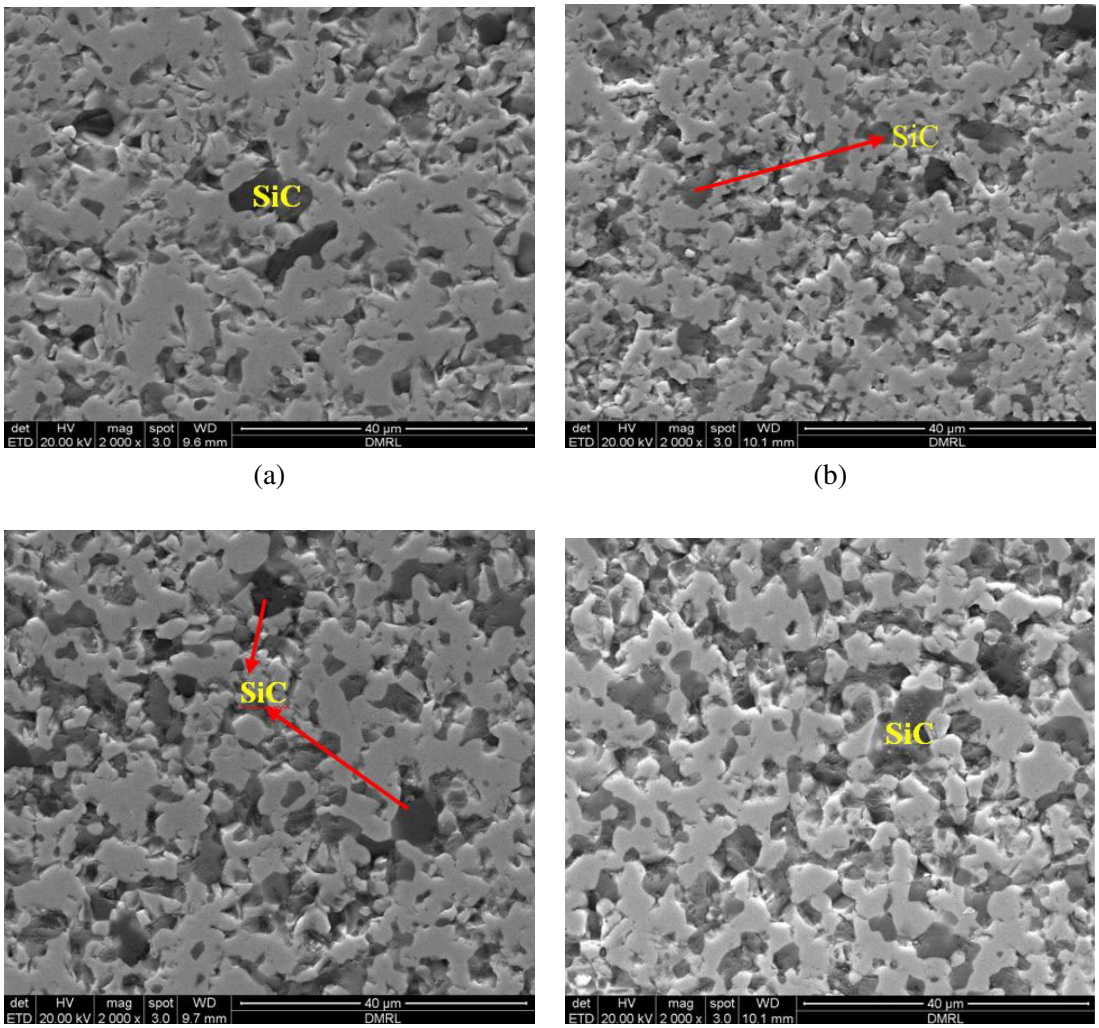

(a) (b)

(c) (d)

Fig. 7. (a) SEM picture of 85% ZrB_2-15% SiC; (b) SEM picture of 80% ZrB_2-20% SiC; (c) SEM picture of 75% ZrB_2-25% SiC; (d) SEM picture of 70% ZrB_2-30% SiC.

A schematic of the instrumentation is shown in Fig. 9. The standard specimen of 55 mm $\times$ 5 mm $\times$ 5 mm is freely supported without rigid fixtures to allow vibrations free of damping and other interferences. Vibrations were induced into the specimens by simple tapping. The piezoelectric probe contacting the specimen detects the mechanical vibrations induced in it and converts it into electrical signal. Read-out device displays the Resonant Frequency (RF) and the frequency analyzer evaluates the signals which have been amplified by the signal amplifier. RF is then found out. The following equation (1) is used to determine the Young's modulus from the values of flexural vibration frequency measured by the RFDA equipment and mass and dimensions of the sample.

$$E = 0.9465 \left[\frac{m f_f^2}{b}\right] \left[\frac{l}{t}\right]^3 T, \tag{1}$$

where f_f is the flexural frequency, m is mass, l is length, b is width, t is thickness and T is the correction coefficient.

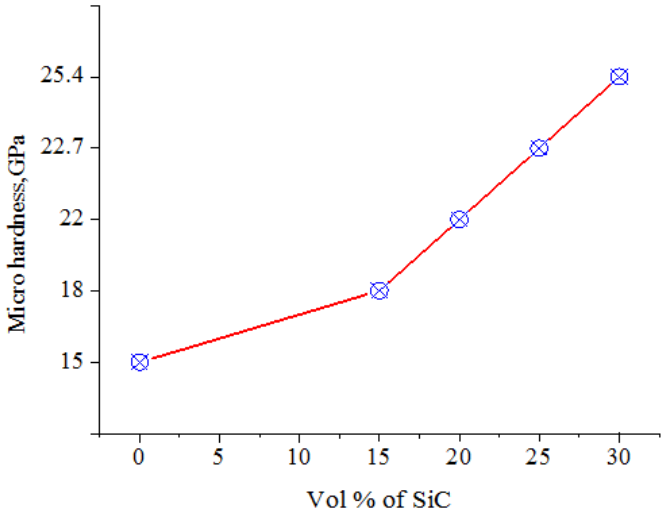

Fig. 8. Micro hardness with different Vol. % SiC.

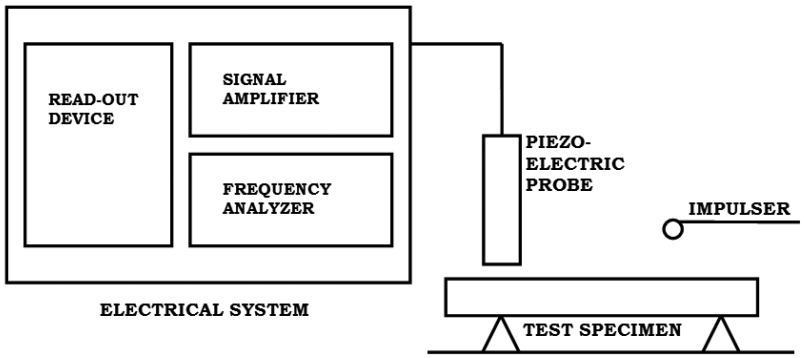

Fig. 9. Schematic of the dynamic modulus measurement system.

Figure 10 shows the variation in Young's modulus and bends strength with respect to Vol. % of SiC. Both the values rise with the volume proportions of SiC and at 20% Vol. of SiC, and both reaches peak values. Hence it may be considered as an optimal volume proportion of the composite.

4. EXPERIMENTAL DESIGNS

This study deals with an experimental investigation on the influence of volume proportions of SiC on machinability of the composites. Table 2 gives the details of experimental design. Each tool performs nine operations in each workpiece. In total, there are 45 operations conducted on each workpiece. MRR, TWR are analyzed. The trends of each response are studied with respect to three major entities which are, pulse on time, pulse off time, aggregate study on the effect of pulse on time, pulse off time and tool.

4.1. Tool Wear Rate

The selection of the most appropriate electrode material is a key decision in the process plan for any sinking EDM job. Drozda [22] emphasized that the tool electrode is responsible for transporting the electrical current to the workpiece. Therefore, electrode material should have the basic properties like electrical and thermal

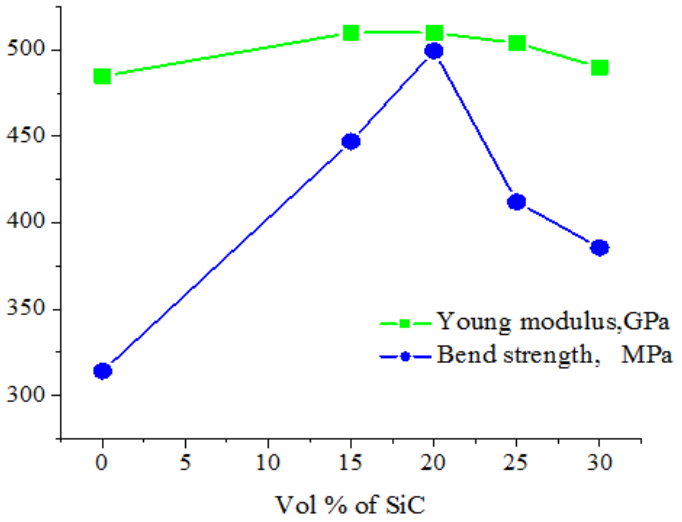

Fig. 10. Bend strength and Young's modulus with Vol. % of SiC.

Table 2. Design of experiments.

Factor/Level	1	2	3	4	5
Pulse on (μs)	4	7	10	–	–
Pulse off (μs)	1	3	5	–	–
Workpiece (No)	85% ZrB_2-15% SiC (1)	80 %ZrB_2-20% SiC (2)	75% ZrB_2-25% SiC (3)	70% ZrB_2-30% SiC (4)	–
Tool (No)	Graphite (1)	Titanium (2)	Niobium (3)	Tantalum (4)	Tungsten (5)

conductivity, a high melting temperature, low wear rate, and resistance to deformation during machining. Properties of different electrode materials and their influence on EDM performance as well as on fabrication of electrodes have been summarized in EDM handbooks [23]. TWR strongly depends on the electrical and thermal properties of the tool material. Evaporation point, melting point, thermal conductivity and thermal diffusivity are the important properties that influence the wear of a tool. The basic requirements of a tool material are high melting and evaporation point in addition to high thermal conductivity. An index is proposed by Yao-Yang Tsai [24] to include the boiling phenomenon for evaluating the erosion property of electrode material in EDM. They stated that volumetric wear ratio of the electrode becomes small for the electrode material with high boiling point, high melting point, and high thermal conductivity. There are four methods known to evaluate the tool wear rate by means of measuring weight, shape, length, and total volume respectively. In this work, the tool wear rate is measured by means of weight basis:

$$TWR = \frac{\text{Weight of tool before machining} - \text{Weight of tool after machining}}{\text{Machining time}}. \quad (2)$$

In this study, Graphite (1), Titanium (2), Niobium (3), Tantalum (4), and Tungsten (5) are selected for experiments. The tools of 2 mm diameter from different materials were fabricated through different techniques like wire cut EDM, diamond grinding and extrusion process.

4.1.1. 85% ZrB_2-15% SiC composites

Generally all the tools show higher TWR at lower pulse duration and vice versa. It is constant (less than 1.5 mg/min) for all tools at 7 μs. W expose lower TWR between 6 and 9 s. GR experiences the lowest TWR for all level of pulse duration.

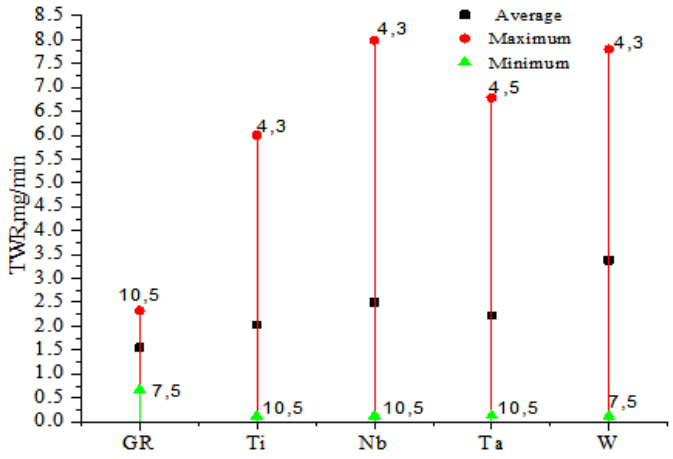

Fig. 11. TWR vs. tool at different pulse conditions for 85% ZrB_2-15% SiC.

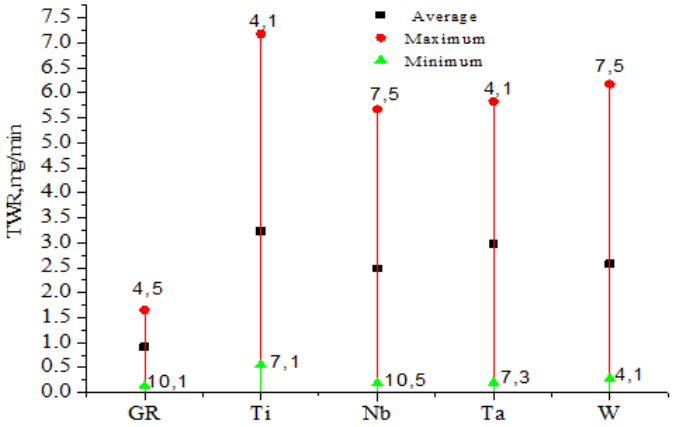

Fig. 12. TWR vs. tool at different pulse conditions for 80% ZrB_2-20% SiC.

GR experience lower TWR than other tools, particularly in pulse off time of 2 to 4 μ s it is less than 1.5 mg/min. Ti shows constant trend at all conditions. Nb exposes higher TWR between 1.5 and 2.8 μs, beyond that it is found to be decreasing. W suffers higher TWR than other tools; particularly during the period of 1.2 to 4.8 μs it is very high. Ta shows less TWR during 2 to 4 μs.

Figure 11 shows the variation in maximum TWR (max-TWR), minimum TWR (min-TWR) and average TWR (avg-TWR) of each tool at different combination of pulse on and pulse off condition (x, y). Ti, Nb and W expose max-TWR at (4, 3). Ti, Nb and Ta leads to min-TWR at (10, 5). GR exposes the lowest max-TWR among all tools at (10, 5). Most of the tool is subjected to severe wear at pulse duration of 4 μs and hence it is not advisable to machine at this condition. Avg-TWR is much less for GR.

4.1.2. 80% ZrB_2-20% SiC composite

Figure 12 shows the detail of variation in wear rate of each tool at different combination of pulse on and pulse off time. The overall highest TWR occurs in Ti at (4, 1). GR undergoes lower max-TWR at (4, 5). Ti encounters the highest avg-TWR and GR encounters the lowest avg-TWR. GR is subjected to overall least TWR at (10, 1). GR proves the lowest constant TWR at all level of pulse duration in the range of

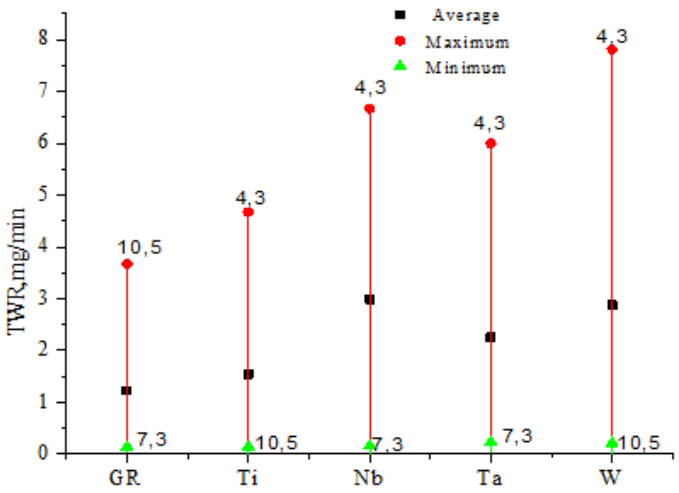

Fig. 13. TWR vs. tool at different pulse conditions for 75% ZrB_2-25% SiC.

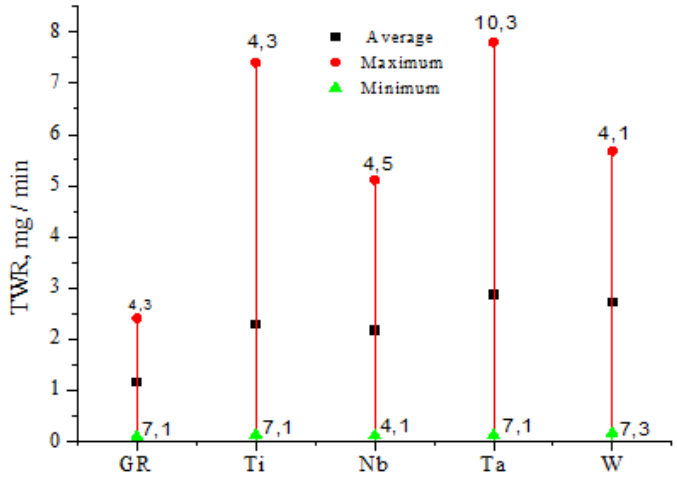

Fig. 14. TWR vs. tool at different pulse conditions for 70% ZrB_2–30% SiC.

1-2 mg/min. In general, except GR all other tools expose higher TWR at lower pulse durations. Ti suffers higher TWR between 4 and 7 µs. Ta undergoes higher wear during 4 to 5 µs.

Constant wear rate is exposed by GR in the range of 1–2 mg/min at all level of pulse off time. Next to GR, Nb shows the lower TWR. In general, except GR all other tools subjected to higher wear at higher pulse off time. Ti undergoes higher TWR during 3 to 5 µs. Ta experience higher TWR during 4 to 5 µs.

4.1.3. 75% ZrB_2-25% SiC composite

At higher pulse on time wear rate is generally less in general. Nb subjected to higher wear on 4 to 5 µs. Ta subjected to higher TWR on 4 to 4.5 µs. In general; at higher pulse off time the TWR is less. GR and Ti encounter lower wears than other tools. At 1 µs, GR subjected to the lowest TWR and Nb experience the highest TWR. W come across the higher wear during 2 to 4 µs pulses off time.

Figure 13 shows the variation in wear of each tool at different combination of pulse on and pulse off condition. Except GR, all other tools are exposed to higher wear rate at (4, 3) and hence this condition is

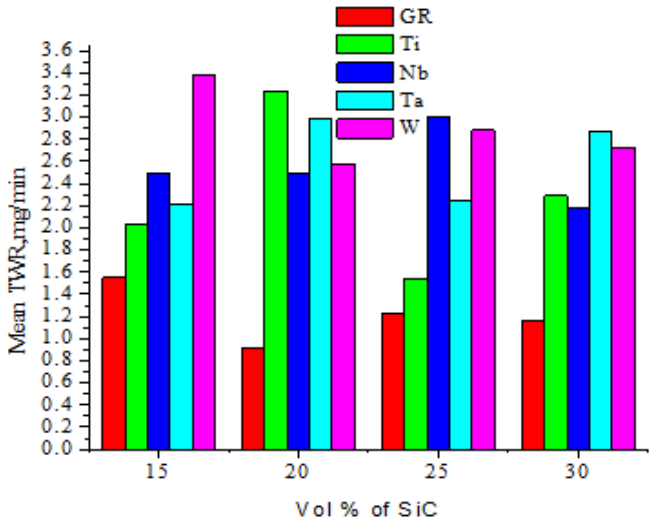

Fig. 15. Mean TWR Imparted by work material.

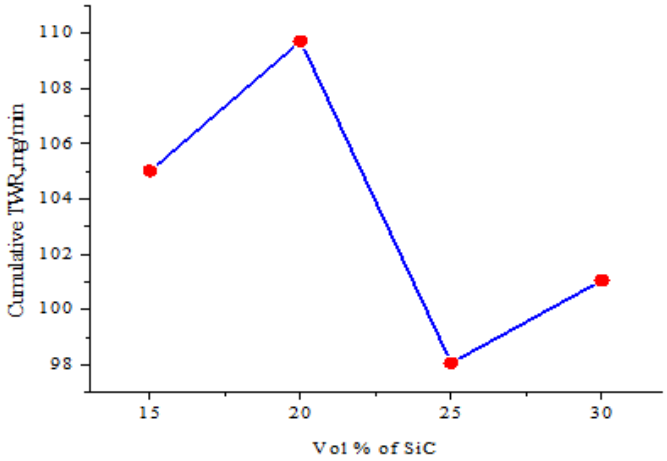

Fig. 16. Cumulative TWR for different Vol. % of SiC.

not generally recommended. GR shows lower max-TWR at (10, 5). Nb and GR subjected to the highest and the lowest avg-TWR respectively. GR, Nb, Ta subjected to min-TWR at (7, 3).

4.1.4. 70% ZrB_2-30% SiC composite

Figure 14 shows the detail of variation in TWR on 30% SiC by each tool at different combination of pulse on and pulse off condition. The overall highest wear rate occurs in Ta at (10, 3) and other tools expose max-TWR at the pulse duration of 4 µs and hence not recommended. This workpiece generates lower TWR than other workpieces. In general TWR is less at pulse duration of 7 µs and thus it is recommended.

Ti and W exposed higher TWR at pulse duration of 4 µs. Ta shows higher TWR on 10 µs. GR, Ti and Nb subjected to TWR less than 1 mg/min at 7 µs. Ta and W always show TWR more than 1 mg/min. In general at around 7 µs all tools possesses lesser wear.

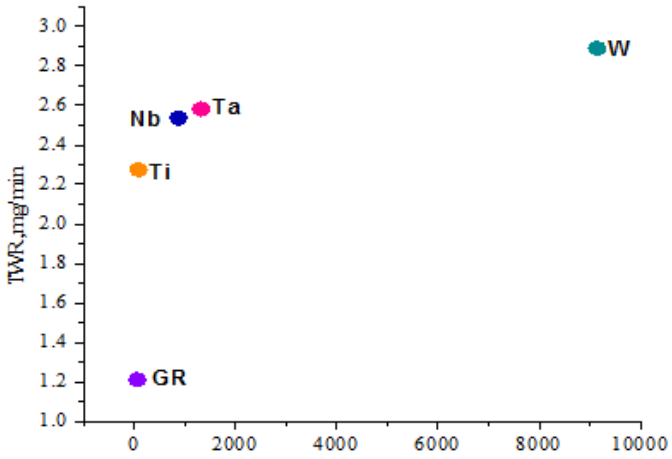

Fig. 17. Cumulative TWR with $\lambda\theta/\rho$, GWΩ.

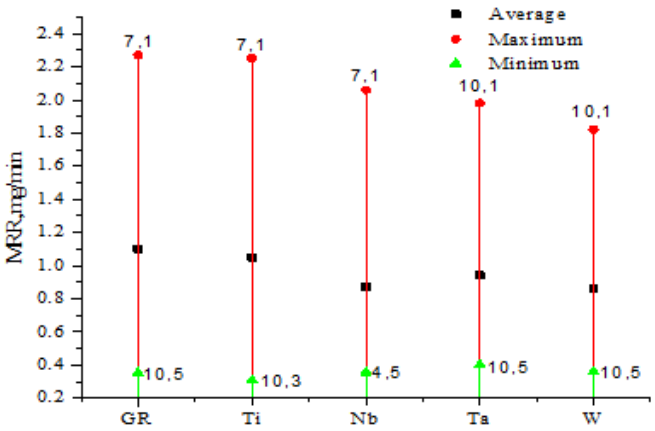

Fig. 18. MRR vs. tool at different pulse conditions for 85% ZrB_2-15% SiC.

It reveals that wear rate is generally less at lower pulse off time and vice versa. GR suffers TWR of less than 1 mg/min at 1 μs. Ti possesses constant level in the range of 2–3 mg/min. Nb possesses TWR of 1–2 mg/min at 1–3 μs then it start increasing. Wear rate is higher for Ta in 2 to 5 μs.

4.1.5. Comparative tool wear study

Mean TWR is calculated for each tool imparted by different workpieces and results are shown in Fig. 15. From this graph it is evident that wear rate of W is higher at workpiece of 15 Vol.% of SiC. Among all tools, GR expose very low wear rate. Ti is subjected to higher wear rate for workpiece of 20 Vol.% of SiC.

Cumulative TWR imparted by each workpiece is presented in Fig. 16. 20 Vol.% of SiC offers higher TWR and 25 Vol.% of SiC offers least TWR.

Figure 17 shows that cumulative TWR increases with respect to $\lambda\theta/\rho$, where λ is the thermal conductivity, θ is the melting point and ρ is the electrical resistivity of the tool.

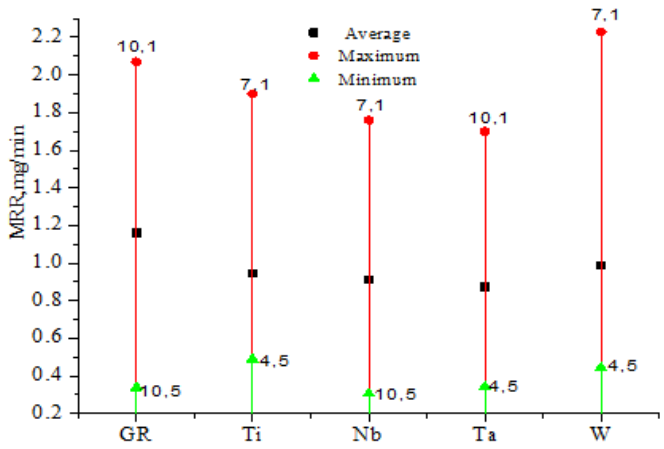

Fig. 19. MRR vs. tool at different pulse conditions for 80% ZrB_2-20% SiC.

4.2. Material Removal Rate

MRR highly influences the production cost. Since the EDM process is the slower process than conventional machining, it becomes essential to concentrate the MRR in order to study the machinability of this material. In this work, material removal rate is calculated based on the weight using

$$MRR = \frac{\text{Weight of workpiece before machining - Weight of workpiece after machining}}{\text{Machining time}}. \quad (3)$$

4.2.1. 85% ZrB_2-15% SiC composites

Each tool performed nine operations, Fig. 18 shows the variation in maximum MRR (max-MRR) produced by each tool, minimum MRR (min-MRR) produced by each tool and average MRR (avg-MRR) produced by each tool materials at different combination of pulse on and pulse off condition. GR, Ti, Nb generate max-MRR at (7 (Pulse on), 1 (Pulse off)) and min-MRR at (10, 5), (10, 3), (4, 5) respectively. Ta and W produce min-MRR at (10, 5) and max-MRR at 10, 1. Most of tool generates maximum MRR at either (10, 1) or (7, 1). GR produces highest avg-MRR and Nb lowest avg-MRR. Min-MRR mostly occurs either at (10, 5) or (10, 3) and hence pulse on time, 10 µs may not be suited for best MRR.

GR produces higher MRR between 4.5 and 10 µs. Ti produces higher MRR during 4 to 9 µs; at 9 µs it starts decreasing. Nb generates best MRR for the period of 5 to 9 µs. Irrespective of pulse duration; Ta and W produce lower MRR in the range of 0.5 to 1 mg/min. All the tools impart higher MRR at lower pulse off time. In particular, GR, Ti makes higher MRR than other tools. Ta makes lower MRR than other tools irrespective of pulse off time.

4.2.2. 80% ZrB_2-20% SiC composite

Figure 19 shows the detail of variation in MRR while machining by each tool at different combination of pulse on and pulse off condition. All tool produce max-MRR at pulse off time of 1 µs hence it is recommended for higher MRR. Ti, Nb and W generate max-MRR at (7, 1). Ta produces lower max-MRR at (10, 1) than other tools. GR produces highest avg-MRR and Ta produces the lowest avg-MRR. All tools produce lower MRR at pulse off time of 5 µs and hence may not be best suited for higher MRR.

GR Produces higher MRR between pulse on time of 7 and 10 µs. At 7 µs all the tools produce higher MRR. In general, MRR at 10 µs is greater than at 4 µs. Ta produces lower MRR than other tools.

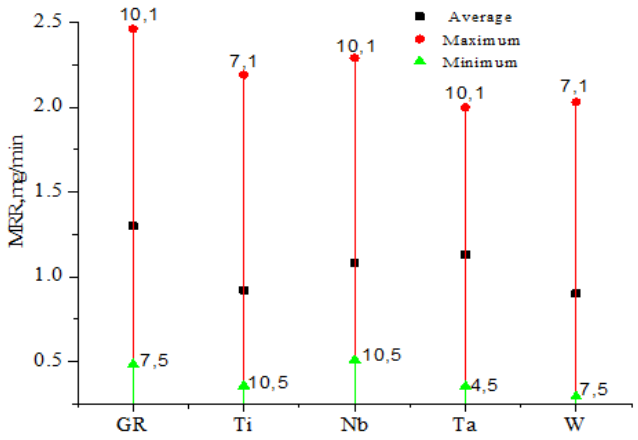

Fig. 20. MRR vs. tool at different pulse conditions for 75% ZrB_2-25% SiC.

GR produces highest MRR than others; particularly the pulse off time between 1 and 3 μs it makes in the range of 1.25–1.5 mg/min. Ta produces the lowest MRR than other tools. In general, at higher pulse off time all tools produce lower MRR.

4.2.3. 75% ZrB_2-25% SiC composite

Figure 20 shows the variation in MRR generated by each tool at different combination of pulse on and pulse off condition. Most of the tools produce max-MRR at either (10, 1) or (7, 1). The overall highest MRR is generated by GR. Ta produces lower max-MRR at (10, 1). GR produces the highest avg-MRR and Ti produces the lowest avg-MRR. W generates the overall least MRR at (7, 5). Least MRR is generated at pulse off time of 5 μs hence may not be best suited for higher MRR.

Pulse duration of 4–5 μs of all the tools produce same MRR in the range of 0.5–1 mg/min. GR produces higher MRR between 9 and 10 μs. Ta produces higher MRR during 9.5 to 10 μs.

In general, all tools produce higher MRR at low pulse off conditions vice versa. GR produces higher MRR through 1 to 2.5 μs. Nb creates higher MRR between 1 and 1.5 μs. At higher pulse off conditions the entire tools generate the same MRR in the range of 0.5–1 mg/min.

4.2.4. 70% ZrB_2-30% SiC composite

Figure 21 shows the variation in MRR on 30% SiC by each tool at different combination of pulse on and pulse off condition. Except W, all other tools produce higher MRR at (7, 1) and hence this condition is recommended. W produces higher MRR at (7, 3). GR produces the highest avg-MRR and Ta the lowest avg-MRR. Ta generates the overall least MRR at (7, 3). Nb generates the highest min-MRR at (4, 3).

GR produces higher MRR during 6 to 10 μs of pulse on time. Nb produces higher MRR between 7 and 10 μs. W creates higher MRR during 5 to 8 μs.

In general, MRR is more at lower pulse off condition and vice versa. Higher volume of material is removed by GR in the wide range of pulse off timing (1–4 μs). Nb, Ti produce very high MRR during 1 to 1.5 μs and after this range of pulse off time, both tools started producing lower MRR.

4.2.5. Comparative study on material removal rate

Each tool performs nine operations on each workpiece, so average of nine value of each response is taken for comparative study. For a particular workpiece, each tool performs 9 experiments with three levels of pulse on and pulse off time. Mean MRR produced by each tool is calculated and plotted against workpiece

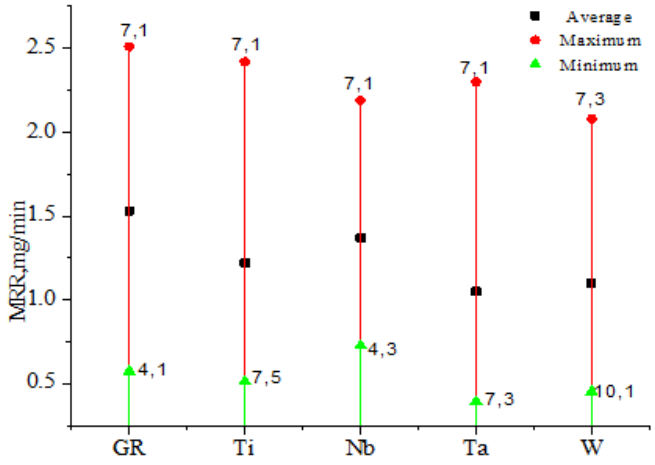

Fig. 21. MRR vs. tool at different pulse conditions for 70% ZrB_2–30% SiC.

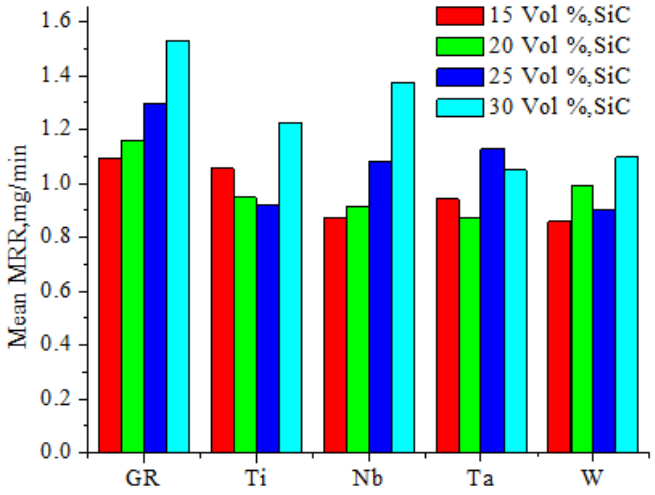

Fig. 22. Mean MRR imparted by tool material.

which is shown in Fig. 22. All tools, except Ta, produce better MRR with workpiece of 30 Vol.% of SiC. Ta produces higher MRR at workpiece of 25 Vol.% of SiC. GR makes higher MRR at all the workpieces. Next to GR, Nb makes higher MRR.

5. CONCLUSIONS

Monolithic ZrB_2 and ZrB_2-SiC composites are prepared by means of a powder metallurgy route. Nearly 100% of density is achieved on all samples. Uniformity in distribution of the reinforcing element is observed using SEM analysis. Bend strength, micro hardness test are conducted. Bend strength is higher for 20% Vol. of SiC. Hardness gets increased with an increase in % Vol. of SiC. MRR of the workpiece increases with an increase in Vol. % of SiC. All the tools, except tantalum, produce better MRR with the workpiece of 30 Vol.% of SiC. Ta produces higher MRR with the workpiece of 25 Vol.% of SiC. Graphite produces higher MRR for all the workpieces. Next to Graphite, Niobium produces higher MRR.

Tool wear rate decreases with an increase of $\lambda\theta/\rho$, where λ is the thermal conductivity of the tool, θ is the melting point of the tool and ρ is the electrical resistivity of the tool. All the tools, except tantalum, produce better MRR with the workpiece of 30 Vol.% of SiC. Ta produces higher MRR with the workpiece of 25 Vol.% of SiC. Graphite produces higher MRR for all the workpieces. Next to Graphite, Niobium produces higher MRR. TWR is less for Graphite against all other workpieces. Generally, the workpiece of 20% Vol. of SiC imparts higher TWR for all the tools.

REFERENCES

1. Abu Zeid, O.A., "On the effect of electro discharge machining parameters on the fatigue life of AISI D6 tool steel", *Journal of Materials Processing Technology*, Vol. 68, No. 1, pp. 27–32, 1997.
2. Guo, S.Q., Yang, J.M., Tanaka, H. and Kagawa, Y., "Effect of thermal exposure on strength of ZrB_2-based composites with nano-sized SiC particles", *Composites Science and Technology*, Vol. 68, No. 14, pp. 3033–3040, 2008.
3. Hwa Yan, B. and Chung Wang, C., "The machining characteristics of Al2O3/6061Al composite using rotary electro-discharge machining with a tube tool", *Journal of Materials Processing Technology*, Vol. 95, No. 1, pp. 222–231, 1999.
4. Jahan, M.P., Wong, Y.S. and M. Rahman, M., "A study on the fine-finish die-sinking micro-EDM of tungsten carbide using different tool materials", *Journal of Materials Processing Technology*, Vol. 209, No. 8, pp. 3956–3967, 2009.
5. Zhu, S., Fahrenholtz, W.G., Hilmas, G.E. and Zhang, S.C., "Pressureless sintering of carbon-coated zirconium diboride powders", *Materials Science and Engineering: A*, Vol. 59, No. 1, pp. 167–171, 2007.
6. Zhang, H., Yan, Y., Huang, Z., Liu, X. and Jiang, D., "Pressureless sintering of ZrB_2-SiC ceramics: The effect of B_4C content", *Scripta Materialia.*, Vol. 60, No 7, pp. 559–562, 2009.
7. Wang, X.G., Guo, W.M. and Zhang, G.J., "Pressureless sintering mechanism and microstructure of ZrB_2-SiC ceramics doped with boron", *Scripta Materialia.*, Vol. 61, No. 2, pp. 177–180, 2009.
8. Lawn, B.R., *Fracture of Brittle Solids*, Cambridge University Press, Cambridge, UK, 1993.
9. Suryanarayana, C., "Mechanical alloying and milling", *Progress in material science*, Vol. 46, No. 1, pp. 1–184, 2001.
10. Schwartz, M.M., "Engineering applications of ceramic materials", *American Society of Metals*, Metals Park, Ohio, 1985.
11. Upadhya, K., Yang, J.M. and Hoffman, W.P., "Materials for ultrahigh temperature structural applications", *American Ceramic Society Bulletein*, Vol. 76, No. 12, pp. 51–56, 1997.
12. Fahrenholtz, W.G., Hilmas, G.E., Talmy, I.G. and Zaykoski, J.A., "Refractory diborides of zirconium and hafnium", *Journal of American Ceramic Society*, Vol. 90, No. 5, pp. 1347–1364, 2007.
13. Chamberlain, A.L., Fahrenholtz, W.G., Hilmas, G.E. and Ellerb, D.T., "High-strength zirconium diboride-based ceramics", *Journal of American Ceramic Society*, Vol. 87, No. 6, pp. 1170–1172, 2004.
14. Tripp, W.C., Davis, H.H. and Graham, H.C., "Effect of an SiC addition on the oxidation of ZrB_2", *Journal of Electrochemical Society*, Vol. 52, No. 8, pp. 612–616, 1973.
15. Hwang, S.S., Vasiliev, A.L. and Padture, N.P., "Improved processing and oxidation resistance of ZrB_2 ultra-high temperature ceramics containing SiC nanodispersoids", *Material Science and Engineering: A*, Vol. 464, No. 1, pp. 216–224, 2007.
16. Cutler, R.A., "Engineering property of borides in ceramics and glasses", in S.J. Schneider (Eds.), *Engineered Materials Handbook*, ASM International, Materials Park, Vol. 4, pp. 787–803, 1992.
17. Monteverde, F., Bellosi, A. and Scatteia, L., "Processing and properties of ultra-high temperature ceramics for space applications", *Materials Science and Engineering*, Vol. 485, No. 1, pp. 415–421, 2008.
18. Son, Seong Min, Lim, Han Seok, Kumar, A.S. and Rahman, M., "Influences of pulsed power condition on the machining properties in micro EDM", *Journal of Materials Processing Technology*, Vol. 190, No. 23, pp. 73–76, 2007.
19. Yaakob, M.M.Y.B., *Electrical Discharge Machining-Die Sinking*, Universiti Tun Hussein on Malaysia (UTHM), 2008.

20. Van Tri, N., *Electrical Discharge Machining of Aluminum Alloy Using Classical Design of Experiment Approach*, Master Thesis, Universiti Teknologi Malaysia, 2002.
21. Qiang Liu, Wenbo Han and Jiecai Han, "Influence of SiCnp content on the microstructure and mechanical properties of ZrB_2-SiC nanocomposit", *Scripta Materialia*, Vol. 63, pp. 581–584, 2010.
22. Drozda, T.J., *Tool and Manufacturing Engineers Handbook: Machining*, Vol. 5, Society of Mechanical Engineers, USA, 1998.
23. Roger Kern Sinker electrode material selection. EDM Today, July/August 2008.
24. Yao-Yang Tsai and Takahisa Masuzawa, "An index to evaluate the wear resistance of the electrode in micro-EDM", *Journal of Materials Processing Technology*, Vol. 149, No. 1, pp. 304–309, 2004.
25. Sivasankar, S., *Machinablility Studies on Electrical Discharge Machining of Hot Pressed ZrB_2-SiC Composites*, PhD Thesis, 2014.